

# Analytical transfer function for the nonlinear response of a resonant medium in the spatio-temporal Fourier-transform domain

MEHJABIN S. MONJUR,<sup>1,\*</sup> MOHAMED F. FOUDA,<sup>1</sup> AND SELIM M. SHAHRIAR<sup>2</sup>

<sup>1</sup>Department of Electrical Engineering and Computer Science, Northwestern University, Evanston, Illinois 60208, USA

<sup>2</sup>Department of Physics and Astronomy, Northwestern University, Evanston, Illinois 60208, USA

\*Corresponding author: mehjabin@u.northwestern.edu

Received 18 August 2016; revised 25 November 2016; accepted 20 December 2016; posted 21 December 2016 (Doc. ID 274081); published 18 January 2017

The nonlinear response of a resonant medium has many applications. To model and find the response of such a medium requires solving the Schrödinger equation (SE), which is a computationally extensive task. In this paper, we develop an analytical model to find the response of a resonant medium due to an applied field by employing the spatio-temporal Fourier-transform (STFT)-domain-based transfer function. A key feature of this approach is the use of the resonant excitation approximation (REA), which amounts to assuming that a group of atoms (or other quantum systems) within a volume element in the STFT domain are excited by only the corresponding volume element in the STFT domain of the field. We first derive the one-dimensional transfer function using an inhomogeneously broadened atomic medium under the REA. Then, we develop the three-dimensional transfer function and show that the analytical model agrees closely with the results obtained via an explicit simulation of the atomic response. As a practical example of the analytical model, we show that it can be used to model a spatio-temporal-correlator-based automatic event recognition system at a speed that is many orders of magnitude faster than solving the SE. © 2017 Optical Society of America

**OCIS codes:** (070.4340) Nonlinear optical signal processing; (070.4550) Correlators.

<https://doi.org/10.1364/JOSAB.34.000397>

## 1. INTRODUCTION

For a given density, resonant media provide the strongest nonlinear interactions [1–4]. Typical examples of such media include rare-earth doped solids [5–7] and atomic vapors [8,9]. The nonlinear response of a resonant medium can be found by numerically solving the quantum mechanical density matrix equations, or simply the Schrödinger equation (SE), if dissipative processes can be ignored. However, this approach is time consuming and cumbersome and, most importantly, does not, in many cases, provide insight into the general characteristics of the response of the medium, especially for a field with complicated patterns in the spatio-temporal Fourier transform (STFT) domain. In this paper, we develop an approach that enables one to determine analytical expressions for the transfer function of such a medium in the STFT domain. We show that the results obtained by applying this approach agree well with those found via exact numerical integration of the quantum mechanical equations of evolution. As a practical example of the utility of this approach, we use it to determine the response of a spatio-temporal-correlator (STC)-based automatic event recognition (AER) [10–12] system in a transparent manner and at a speed

that is many orders of magnitude faster than direct numerical integration.

The paper is organized as follows. In Section 2, first we derive the analytical transfer function of an inhomogeneously broadened atomic medium (AM) due to a sequence of one-dimensional temporal pulses. Then, we develop the three-dimensional transfer function of the system. In Section 3, we present simulation results showing that the analytical model agrees well with the results obtained by solving the SE. Concluding statements are made in Section 4.

## 2. ANALYTICAL MODEL OF THE RESPONSE OF A RESONANT MEDIUM

To illustrate the basic tenets of the nonlinear response of a resonant medium, consider, for example, an AM (e.g., a hot vapor cell) with specified extents in the  $x$ - $y$  plane and negligible thickness in the  $z$ -direction. We assume further that it has significant inhomogeneous broadening and a finite granularity in the  $x$ - $y$  plane. Under these assumptions, the three-dimensional space occupied by this medium in the STFT domain can be represented by a volume, such as the one in Fig. 1(a). Here,

$k_x$  and  $k_y$  are the spatial frequencies, and  $\omega$  is the temporal frequency. The actual shape of this volume would, of course, depend on the nature and extent of the inhomogeneous broadening and the size and the granularity of the medium in the  $x$ - $y$  plane. Next, consider the corresponding representation of a pulsed optical field in the paraxial limit. In Fig. 1(b), we show an arbitrary lump as the representation of this field in the STFT domain. Again, of course, the actual shape of this lump would depend on the spatial and temporal properties of this pulse.

Consider now an arbitrary volume element of the STFT representation of the field. In general, this volume element will interact with the whole volume of the STFT representation of the medium. However, limited by a very small volume element, the power in this element is so small that one can make the resonant excitation approximation (REA). Explicitly, the REA means we consider only the interaction between volume elements that have the same coordinates at the center. This enables us to determine a transfer function for each volume element of the excitation field. The overall response can then be found by simply integrating the transfer function over the volume of the STFT representation of the field and the spectral distribution of the atoms.

As we have noted above, the quantum mechanical equation of evolution is simply the SE if dissipative processes are negligible. An important example of such a situation occurs when optically off-resonant two-photon (Raman) excitations are applied to a  $\Lambda$ -type system [13,14]. As has been shown, such a system can be modeled as a dissipation-free two-level system. In this case, we will show that an analytical expression for the transfer function can be found. In a more general case, where the dissipation cannot be ignored, one must use the Liouville equation for the density matrix. In such a case, the transfer function itself has to be determined numerically, as described in more detail later. Nonetheless, it would still allow computation at a rate that is orders of magnitude faster than direct numerical integration. In this paper, we focus our discussion on the case where an analytical expression for the transfer function can be found.

To keep the exposition of the basic feature of the analysis simple, we first consider a field that corresponds to a delta function in the spatial frequency domain and has a spread in the temporal frequency domain only. A specific example of such

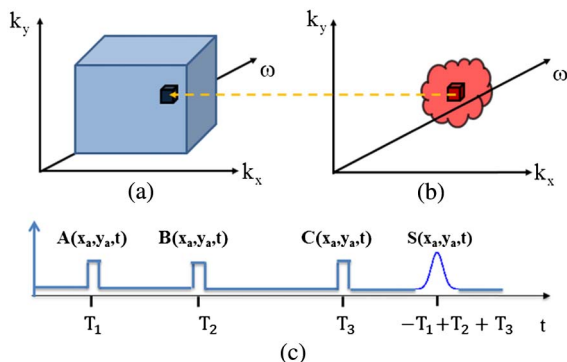


**Fig. 1.** STFT representation of (a) the AM and (b) the three-dimensional electric field. (c) Sequence of pulses in the SPE process.

a field is shown in Fig. 1(c), consisting of three pulses, with infinite and uniform spatial extents in the  $x$ - and  $y$ -directions. We assume that the AM has inhomogeneous broadening centered at frequency  $\omega_L$ , with a width that is significantly larger than the spectral width of each of the three pulses. Furthermore, we assume that the carrier frequencies of these pulses are also  $\omega_L$ . Let us assume further that each of the last two pulses is a so-called  $\pi/2$  pulse, meaning that, by itself, each pulse would create an equal superposition of the ground and the excited state of an atom with a resonance frequency of  $\omega_L$ , starting in the ground state. In that case, this pulse sequence corresponds to the so-called stimulated photon echo [15,16] (SPE) process. Specifically, the response of the AM generates the echo pulse, which is a temporally mirrored version of the first pulse. The SPE process can be viewed as a temporal correlator (TC) [17–19], with the echo pulse representing the correlation peak. We denote the three temporal signals as  $A(t)$ ,  $B(t)$ , and  $C(t)$ . More explicitly, these functions represent the complex envelope of the electric field amplitude, with a central frequency of  $\omega_L$ . Explicitly, we can write  $E_Q(t) = Q(t) \exp(i(\omega_L t - kz)) + cc = |Q(t)| \exp(i\phi_Q)$ , where  $Q = A, B, C$ .

After applying the rotating wave approximation and the rotating wave transformation [13] (which is augmented to transform out the common phase factor  $kz$  as well), the effective Hamiltonian for each of these fields can be expressed as  $H_Q(t)/\hbar = \omega|2\rangle\langle 2| + \Omega_Q(t)/2|1\rangle\langle 2| + \Omega_Q^*(t)/2|2\rangle\langle 1|$ , where the complex and time-dependent Rabi frequency for each field is given by  $\Omega_Q(t) = \mu Q(t) = |\Omega_Q(t)| \exp(i\phi_Q)$ , ( $Q = A, B, C$ ), with  $\mu$  being the dipole moment of the two-level atom, and the detuning of the center frequency of the laser ( $\omega_L$ ) from the resonance frequency of the atom ( $\omega_{\text{Atom}}$ ) being defined as  $\omega \equiv \omega_{\text{Atom}} - \omega_L$ .

As shown in Fig. 1(c), the three temporal signals have finite durations in time and are separated from one another. Specifically, we assume that the three signals,  $A$ ,  $B$ , and  $C$ , arrive at the AM at  $t = T_1$ ,  $T_2$ , and  $T_3$ , respectively. Therefore, the Rabi frequencies seen by the AM can be expressed as  $\Omega_q(t) = \mu q(t) = |\Omega_q(t)| \exp(i\phi_Q)$ ; ( $Q = A, B, C$ ;  $q = a, b, c$ ), where  $a(t) = A(t - T_1)$ ;  $b(t) = B(t - T_2)$ ;  $c(t) = C(t - T_3)$ . Before proceeding further, we define explicitly the time domain Fourier transform (FT),  $\tilde{g}(\omega)$ , of a function  $g(t)$  as  $\tilde{g}(\omega) = (1/\sqrt{2\pi}) \int_{-\infty}^{\infty} g(t) \exp(i\omega t) dt$ . From this definition, it then follows immediately that  $\tilde{\Omega}_a(\omega) = \mu \tilde{a}(\omega) = \mu \tilde{A}(\omega) \exp(i\omega T_1)$ ;  $\tilde{\Omega}_b(\omega) = \mu \tilde{b}(\omega) = \mu \tilde{B}(\omega) \exp(i\omega T_2)$ ;  $\tilde{\Omega}_c(\omega) = \mu \tilde{c}(\omega) = \mu \tilde{C}(\omega) \exp(i\omega T_3)$ .

In the time domain, the atoms see the pulses at different times. However, the equivalent picture in the frequency domain is that the atoms see the Fourier components of all the pulses simultaneously during the time window within which all three pulses are present. Thus, for  $t \geq T_3$ , the response of the AM can be computed by assuming that it has interacted with all the fields simultaneously. To evaluate this response, we denote first as  $N(\omega)$  the distribution of the atomic frequency detunings (i.e., the inhomogeneous broadening). Thus, the quantity  $N(\omega)d\omega$  represents the number of atoms that have detunings ranging from  $\omega - \Delta\omega/2$  to  $\omega + \Delta\omega/2$ , representing a spectral band of very small width  $\Delta\omega$ . In the

spectral domain view, a good approximation (the REA) to make is that the atoms interact only with those components of the field that are resonant with the atoms within a small band, justified by the fact that the spectral component within a vanishingly small band is very small. Thus, the SE for the amplitude of this band of atoms, in the rotating wave frame, is given by

$$\frac{\partial}{\partial t} \begin{bmatrix} C_1(\omega) \\ C_2(\omega) \end{bmatrix} = -i \begin{bmatrix} 0 & \tilde{\Omega}'(\omega)/2 \\ \tilde{\Omega}'^*(\omega)/2 & 0 \end{bmatrix} \begin{bmatrix} C_1(\omega) \\ C_2(\omega) \end{bmatrix}, \quad (1)$$

where the net, complex Rabi frequency within this band is given by  $\tilde{\Omega}(\omega) = \tilde{\Omega}_a(\omega) + \tilde{\Omega}_b(\omega) + \tilde{\Omega}_c(\omega) = \mu(\tilde{a}(\omega) + \tilde{b}(\omega) + \tilde{c}(\omega)) \equiv |\tilde{\Omega}(\omega)| \exp(i\phi(\omega))$ , and we have defined  $\tilde{\Omega}'(\omega) \equiv \tilde{\Omega}(\omega)\Delta\omega$ .

The conditions under which the approximation underlying Eq. (1) is valid are as follows. If the optical fields are applied for a duration of  $T$ , then it has a spectral width of the order of  $\sim 1/T$ . Let us denote by  $\Omega$  the peak Rabi frequency in the time domain. Thus, the strength of the Rabi frequency causing the resonant excitation for each of these bands of atoms is  $\sim \Omega \cdot \Delta\omega \cdot T$ . Consider now the excitation of one band by the component of the fields that are detuned by a frequency  $\Delta\omega$ . If we assume the condition that  $\Omega \cdot T \ll 1$ , then it follows that  $\Omega \cdot \Delta\omega \cdot T \ll \Delta\omega$ . The peak amplitude of the excited state due to this detuned excitation is then given approximately by the ratio of the effective Rabi frequency to the detuning, which is  $\Omega \cdot T$ . Thus, it follows that the REA underlying Eq. (1) is valid as long as  $\Omega \cdot T \ll 1$ , which is assumed to be the case for the system under consideration in this paper. We also note that such an approach for describing the evolution in bands has been employed in other contexts as well; see, for example, Refs. [20,21].

Assuming that all the atoms are in the ground state before the first pulse is applied, the solution for this equation, physically valid for  $t \geq T_3$ , is given by  $C_1(\omega) = \text{Cos}[|\tilde{\Omega}'(\omega)|t/2]$ ;  $C_2(\omega) = -i \text{Sin}[|\tilde{\Omega}'(\omega)|t/2] \exp(-i\phi(\omega))$ . The amplitude of the electromagnetic field produced by the atoms in this band is proportional to the induced dipole moment, which, in turn, is proportional to the induced coherence, given by

$$\begin{aligned} \rho_{12}(\omega, t) &= C_1 C_2^* \exp(-i\omega_{\text{atom}}t) = C_1 C_2^* \exp(-i\omega_L t - i\omega t) \\ &= (i/2) \exp(-i\omega_L t) \text{Sin}[|\tilde{\Omega}'(\omega)|t] \exp(-i\omega t) \exp(i\phi(\omega)). \end{aligned} \quad (2)$$

As we argued above, the component of the Rabi frequency within a very small band is very small, so we can make use of the approximation that  $\text{Sin}(\theta) \approx \theta - \theta^3/6$ . Noting that the interaction occurs for a time window of duration  $T \approx T_3 - T_1$ , we can thus write that  $\rho_{12}(\omega, t) \approx (i/2) \exp(-i\omega_L t) \times [|\tilde{\Omega}'(\omega)T - |\tilde{\Omega}'(\omega)|^2 \tilde{\Omega}'(\omega) T^3/6] \exp(-i\omega t)$ . The signal (i.e., the electric field) produced by all the atoms can be expressed as

$$\begin{aligned} \Sigma(t) &= \alpha \exp(-i\omega_L t) \int_{-\infty}^{\infty} d\omega N(\omega) [|\tilde{\Omega}(\omega)T \\ &\quad - |\tilde{\Omega}'(\omega)|^2 \tilde{\Omega}'(\omega) T^3/6] \exp(-i\omega t), \end{aligned} \quad (3)$$

where the proportionality constant,  $\alpha$ , depends on the dipole moment of the two-level atom and the density of the AM. To

extract the essential result, we assume that the width of the atomic spectral distribution is very large compared to that of  $\tilde{\Omega}(\omega)$ , so  $N(\omega)$  can be replaced by a constant,  $N$ . Furthermore, we define  $\Sigma'(t) = \Sigma(t) \exp(i\omega_L t)$  as the envelope of the signal centered at the laser frequency, and  $\beta = -\alpha N$ , so we can write

$$\Sigma'(t) = \beta \int_{-\infty}^{\infty} d\omega [|\tilde{\Omega}'(\omega)|^2 \tilde{\Omega}'(\omega) T^3/6 - \tilde{\Omega}'(\omega) T] \times \exp(-i\omega t). \quad (4)$$

Note that the time-dependent value of the off-diagonal density matrix element  $\rho_{12}(t)$ , integrated over all atoms, is simply proportional to this signal,  $\rho_{12}(t) = \xi \Sigma(t)$ , where  $\xi$  is a proportionality constant. This, of course, is proportional to the density matrix element in the rotating wave frame

$$\tilde{\rho}_{12}(t) \equiv \rho_{12} e^{i\omega_L t} = \xi \Sigma(t) e^{i\omega_L t}. \quad (5)$$

The linear terms in Eq. (3) represent the so-called free-induction decay, which occurs immediately after each pulse leaves the AM, as can be shown easily, and does not contribute to the correlation signal. Since the net Rabi frequency has three components corresponding to the three pulses, there will be a total of twenty-seven components corresponding to the nonlinear term. However, some of these terms are identical to one another, except for the numerical coefficients, leading to eighteen distinct terms. These are illustrated in Fig. 2, where the coefficient in front of each term indicates the number of times it occurs. These terms can first be divided into two categories: causal and acausal. The acausal terms occur at a time that is earlier than the time of application of at least one of the three constituent input signals. To eliminate the appearance of such acausal terms, it is necessary use Laplace transforms rather than FTs in formulating the frequency domain analysis, a fact well known in the field of signal processing [22]. However, for the problem we are considering here (namely, the spatio-temporal correlator; STC), it is essential to use FTs in the spatial domain. In order to elicit and exploit the unified view of the STC as a device that adds the temporal dimension to the spatial ones with essentially identical notations and interpretations, we are forced to make use of the FT for the temporal dynamics.

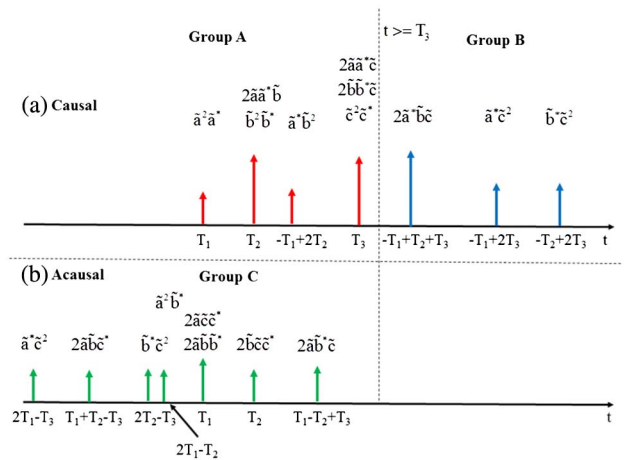


**Fig. 2.** List of nonlinear terms from third-order expansion. (a) The causal terms. (b) The acausal terms [Group A: causal and appearing at  $t \leq T_3$ ; Group B: acausal; Group C: causal and appearing at  $t > T_3$ ].

This approach is fully valid as long as it is understood that the acausal terms that appear due to the use of the FT are unphysical and must be discarded while determining the actual response of the system.

The causal category can be broken up into two groups: those appearing at  $t \leq T_3$ , and those appearing after  $t > T_3$ . For reference, we thus have three different groups of signals, designated as follows: Group A: Causal and appearing before or at  $T_3$ ; Group B: Acausal; and Group C: Causal and appearing after  $T_3$ . This grouping is indicated in the caption of Fig. 2. In grouping these terms, we have assumed that  $(T_2 - T_1) < (T_3 - T_2)$ . Under the assumptions made here in deriving these results, the only physically meaningful terms are those in Group C, since we are calculating the response of the atoms to the combined field of all three pulses. These correspond to inverse FT of  $\tilde{a}^* \tilde{b} \tilde{c}$ ,  $\tilde{b}^* \tilde{c}^2$ ,  $\tilde{a}^* \tilde{c}^2$ , appearing at time  $t = -T_1 + T_2 + T_3$ ,  $t = -T_2 + 2T_3$ , and  $t = -T_1 + 2T_3$ . The term that corresponds to the desired correlation signal is  $\tilde{a}^* \tilde{b} \tilde{c}$ .

We now consider explicitly the signal produced by the term  $\tilde{a}^* \tilde{b} \tilde{c}$ . It can be expressed as  $\Sigma'_C(t) = [\zeta \mu^3 / 6] \times \int_{-\infty}^{\infty} d\omega [\tilde{a}^*(\omega) \tilde{b}(\omega) \tilde{c}(\omega)] \exp(-i\omega t)$ , where  $\zeta \equiv \beta(T\Delta\omega)^3$ . For simplicity, we now define the normalized signal as  $\sigma(t) \equiv \Sigma'_C \sqrt{2\pi} * 6 / [\zeta \mu^3]$ , so we can write  $\sigma(t) = (1/\sqrt{2\pi}) \int_{-\infty}^{\infty} d\omega [\tilde{a}^*(\omega) \tilde{b}(\omega) \tilde{c}(\omega)] \exp(-i\omega t)$ . It then follows that the FT of the normalized correlation signal is

$$\begin{aligned} \tilde{\sigma}(\omega) &= \tilde{a}^*(\omega) \tilde{b}(\omega) \tilde{c}(\omega) \\ &= \tilde{A}^*(\omega) \tilde{B}(\omega) \tilde{C}(\omega) \exp(j\omega(T_3 + T_2 - T_1)). \end{aligned} \quad (6)$$

If we define  $\tilde{S}(\omega) = \tilde{A}^*(\omega) \tilde{B}(\omega) \tilde{C}(\omega)$ , then it follows that  $S(t)$  is the cross-correlation between  $A(t)$  and the convolution of  $B(t)$  and  $C(t)$ . Since  $A(t)$  is essentially a delta function in time,  $S(t)$  is effectively the convolution of  $B(t)$  and  $C(t)$ . Explicitly, if we consider  $A(t) = A_0 \delta(t)$ , we get  $S(t) = A_0 \int_{-\infty}^{\infty} B(t') C(t - t') dt'$ . If we take into account the finite temporal width of  $A(t)$ , this signal  $S(t)$  will be broadened by this added width. Finally, we note that  $\sigma(t) = S(t - (T_3 + T_2 - T_1))$ , which means that this correlation signal occurs at  $t = T_3 + (T_2 - T_1)$ , as already noted above. Here, we have used an idealized, decay-free two-level system of atoms with inhomogeneous broadening that is larger than the inverse of the temporal resolution of the data stream. As stated earlier, it can be shown that an off-resonant excitation in a three-level system is equivalent to this model [13,14].

### 3. SIMULATION RESULTS AND DISCUSSION

Now we compare the simulation results of the numerical model and the analytical model and verify that both models give essentially the same results. Figure 3(a) shows the sequence of pulses associated with the TC, where a short pulse  $a(t)$  is applied as the writing beam at time  $T_1$ , followed by the query pulse train  $b(t)$  at time  $T_2$ . At time  $T_3$ , the reference pulse train is applied to this memory. The correlation peak is observed in a temporally shift-invariant manner at time  $t = -T_1 + T_2 + T_3$ . The temporal correlation process described above is simulated using the quantum mechanical amplitude equation [13,14], and the result is shown in Fig. 3(b). The simulation of the atomic model has been

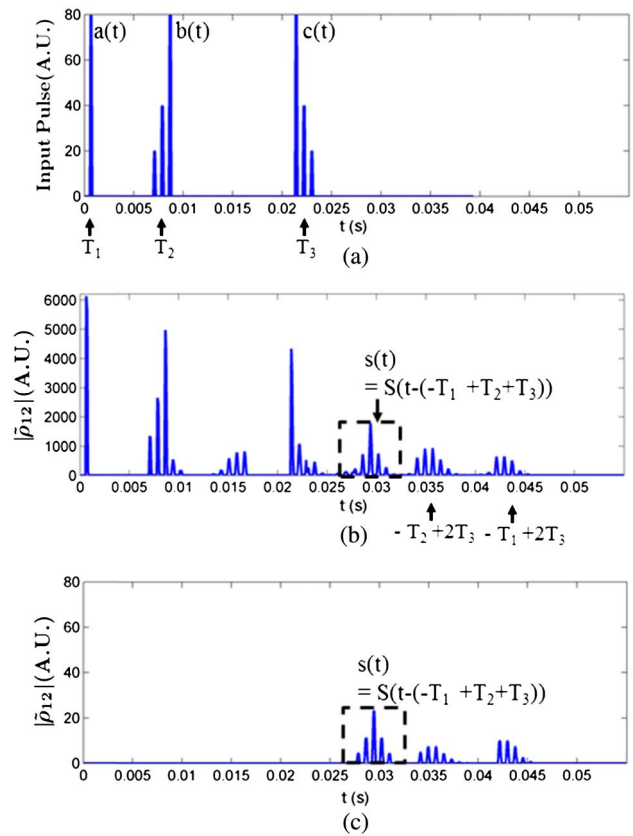


**Fig. 3.** (a) Pulse train associated with the TC. (b) Simulation results of a TC using the numerical model, and (c) the analytical transfer function model. (A.U., arbitrary unit.)

performed in a supercomputer for faster calculation. In addition to the correlation term, other nonlinear terms appear in the simulation; these have been discussed above. In the simulation of a TC using the numerical model in Fig. 3(b), we see that the terms in Group C appear at times  $t = -T_1 + T_2 + T_3$ ,  $t = -T_2 + 2T_3$ , and  $t = -T_1 + 2T_3$ . Here, the desired correlation signal, which is denoted as  $s(t)$ , corresponds to the term  $\tilde{a}^* \tilde{b} \tilde{c}$ , and it appears at time  $t = -T_1 + T_2 + T_3$ , as expected. It should be noted that there is a signal that appears at time  $t = -T_1 + 2T_2$ . Since it appears before  $t = T_3$ , it is of no interest for the temporal correlation process.

To simulate the analytical model, it is necessary to modify the transfer function of Eq. (6) by adding the additional nonlinear terms of Group C. Thus, the modified version of the transfer function can be expressed as

$$\tilde{\sigma}(\omega) = 2\tilde{a}^*(\omega) \tilde{b}(\omega) \tilde{c}(\omega) + \tilde{b}^*(\omega) \tilde{c}^2(\omega) + \tilde{a}^*(\omega) \tilde{c}^2(\omega), \quad (7a)$$

$$\sigma(t) = \text{IFT}\{\tilde{\sigma}(\omega)\}, \quad \text{for } t > T_3, \quad (7b)$$

where the three terms correspond to Group C. The quantity  $\sigma(t)$  is proportional to the signal produced by the system for  $t > T_3$ , under the simplifying assumption that the inhomogeneous broadening is much larger than the spectral spread of the terms in Eq. (7a). It can be shown that this term is proportional to  $\tilde{\rho}_{12}(t)$ , the off-diagonal density matrix element in the

rotating-wave basis. In Fig. 3(c), we have shown that implementing the transfer functions of Eq. (7) essentially yields the same result as the numerical model (for  $t > T_3$ , which is the relevant time span for the correlator), but at a faster simulation time. Note that the other nonlinear terms appearing in this case do not interfere with the final correlation signal.

The architecture for the AER system based on an STC is similar to that of a conventional spatial holographic correlator [10,23,24], except that the write pulse is replaced by a plane wave of a certain duration in space and time. The recording medium is replaced by the inhomogeneously broadened AM. The laser beam is directed to the reflection-mode spatial light modulator (SLM) with a polarizing beam splitter. The SLM reflects a pattern of light that is orthogonally polarized so it passes through the same beam splitter. The pattern produced by the SLM is controlled by the signals applied to it. The lens after the SLM produces the two-dimensional spatial FT of the SLM pattern in the plane of the AM. Similarly, the second lens produces the two-dimensional spatial FT of the field, generated by the AM, in the plane of the detector array. A simplified architecture of the STC is shown in Fig. 4. Here, the signals are generated by modulating the field from a laser with an SLM, for example. We now have three functions containing information:  $A(x, y, t)$ ,  $B(x, y, t)$ , and  $C(x, y, t)$ , where  $(x, y)$  are the rectilinear spatial coordinates in the plane of the SLM. The corresponding signals in the plane of the AM are FT'd in the spatial domain due to the first lens. The signals  $A(x, y, t)$ ,  $B(x, y, t)$ , and  $C(x, y, t)$  are retrieved from the SLM at times  $T_1$ ,  $T_2$ , and  $T_3$ , respectively. We also allow for the situation where each frame might be shifted from the center by an amount  $(x_j, y_j)$ . The corresponding Rabi frequencies in the three-dimensional spectral domain can be expressed as  $\tilde{\Omega}_q(k_x, k_y, \omega) = \zeta \mu \tilde{Q}(k_x, k_y, \omega) \exp(ik_x x_q) \exp(ik_y y_q) \exp(i\omega T_q)$ ; [ $q = a, b, c$ ;  $Q = A, B, C$ ], where  $a(x, y, t) = A(x - x_a, y - y_a, t - T_1)$ ;  $b(x, y, t) = B(x - x_b, y - y_b, t - T_2)$ ;  $c(x, y, t) = C(x - x_c, y - y_c, t - T_3)$ . Thus, the SE for the amplitude in the rotating-wave frame is given by

$$\frac{\partial}{\partial t} \begin{bmatrix} C_1(k_x, k_y, \omega) \\ C_2(k_x, k_y, \omega) \end{bmatrix} = -i \begin{bmatrix} 0 & \tilde{\Omega}(k_x, k_y, \omega)/2 \\ \tilde{\Omega}^*(k_x, k_y, \omega)/2 & 0 \end{bmatrix} \times \begin{bmatrix} C_1(k_x, k_y, \omega) \\ C_2(k_x, k_y, \omega) \end{bmatrix}, \quad (8)$$

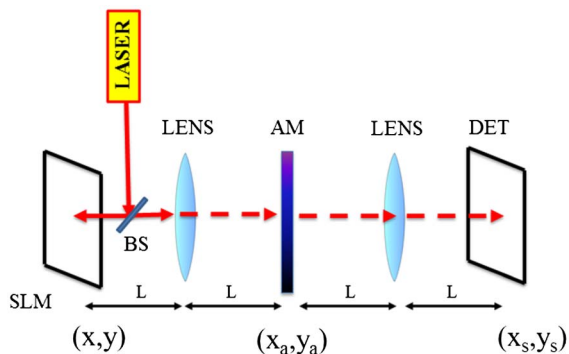


**Fig. 4.** Simplified architecture of the STC. (SLM, spatial light modulator; AM, atomic medium; DET, detector.) See text for details.

where the net, complex Rabi frequency within this band is given by  $\tilde{\Omega}(k_x, k_y, \omega) = \tilde{\Omega}_a(k_x, k_y, \omega) + \tilde{\Omega}_b(k_x, k_y, \omega) + \tilde{\Omega}_c(k_x, k_y, \omega) = \mu(\tilde{a}(k_x, k_y, \omega) + \tilde{b}(k_x, k_y, \omega) + \tilde{c}(k_x, k_y, \omega))$ . Here, we are making a more generalized form of the REA. Specifically, we are assuming that the atoms in the STFT domain volume element  $(k_x - \Delta k_x/2, k_y - \Delta k_y/2, \omega - \Delta\omega/2) \rightarrow (k_x + \Delta k_x/2, k_y + \Delta k_y/2, \omega + \Delta\omega/2)$  interact only with those components of the field that occupy the same volume element. Using the same line of argument and making use of the same set of approximations as presented for the temporal-only case, we then conclude that the normalized signal in the plane of the detector array corresponding to the correlation signal is given by

$$\sigma(x_s, y_s, t) = \frac{1}{[2\pi]^{3/2}} \int_{-\infty}^{\infty} dk_x \int_{-\infty}^{\infty} dk_y \int_{-\infty}^{\infty} d\omega [\tilde{A}^*(k_x, k_y, \omega) \times \tilde{B}(k_x, k_y, \omega) \tilde{C}(k_x, k_y, \omega) \exp(ik_x(x_3 + x_2 - x_1) + ik_y(x_3 + x_2 - x_1)) \exp(i\omega(T_3 + T_2 - T_1))] \times \exp(-i(k_x x_s + k_y y_s + \omega t)). \quad (9)$$

If we consider no shift in the spatial direction, i.e.,  $x_q = y_q = 0$  where  $q = a, b, c$ , then it follows that the three-dimensional FT of the normalized correlation signal is

$$\tilde{\sigma}(k_x, k_y, \omega) = \tilde{A}^*(\omega) \tilde{B}(\omega) \tilde{C}(\omega) \exp(i\omega(T_3 + T_2 - T_1)). \quad (10)$$

If we define  $\tilde{S}(k_x, k_y, \omega) = \tilde{A}^*(k_x, k_y, \omega) \tilde{B}(k_x, k_y, \omega) \tilde{C}(k_x, k_y, \omega)$ , then we see that  $S(x_s, y_s, t)$  is the three-dimensional cross-correlation between  $A(x, y, t)$  and the three-dimensional convolution of  $B(x, y, t)$  and  $C(x, y, t)$ . Since  $A(x, y, t)$  is essentially a delta function in both the temporal and spatial domains (i.e., it is a very short temporal pulse and is a small point signal at the center of the SLM plane),  $S(x_s, y_s, t)$  is effectively the three-dimensional convolution of  $B(x, y, t)$  and  $C(x, y, t)$ . Explicitly, if we consider  $A(x, y, t) = A_0 \delta(x) \delta(y) \delta(t)$ , we get  $S(x_s, y_s, t) = A_0 \int_{-\infty}^{\infty} dt' \int_{-\infty}^{\infty} dx' \int_{-\infty}^{\infty} dy' B(x', y', t') \times C(x_s - x', y_s - y', t - t')$ . Finally, we note that  $\sigma(x_s, y_s, t) = S(x_s, y_s, t - (T_3 + T_2 - T_1))$ , which means that this correlation signal occurs at  $t = T_3 + (T_2 - T_1)$  in the plane of the detector array.

Figure 5 shows the limiting case of the STC where the query event and the database event are each a single frame, and they match exactly in the spatial domain. Specifically, the write pulse,  $A(x, y, t)$ , is applied (centered) at  $t = T_1$ . In the time domain, it is a  $\pi/2$  pulse, while spatially, it is a Gaussian spot (centered) at  $x = 0, y = 0$ . The query image,  $B(x, y, t)$ , is applied (centered) at  $t = T_2$ , and the reference image  $C(x, y, t)$  is applied (centered) at  $t = T_3$ . As expected, a correlation peak appears at  $t = T_2 + T_3 - T_1$ . Here, we can see that the numerical and the analytical models yield essentially identical results, but at a faster simulation time. The numerical model is simulated using a parallel computer [25–27] with 20 processors, whereas the analytical model is simulated using a single processor (Intel Core I7-4600U CPU at 2.1 GHz). However, the simulation time of the analytical model is  $\sim 10^5$  faster than the numerical model. Both models also show additional signals appearing at different times, corresponding to the additional nonlinear interactions, similar to the results

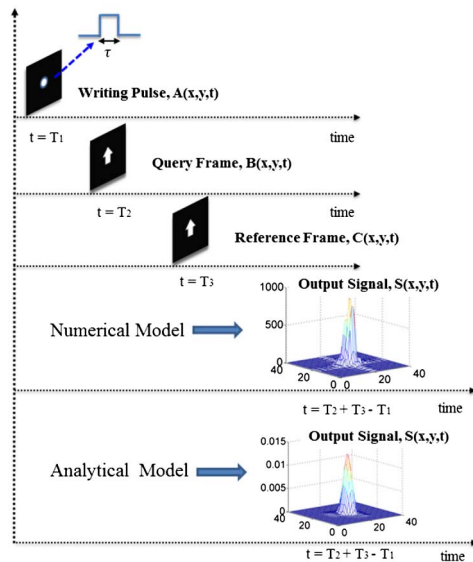


**Fig. 5.** Simulation of the STC using the numerical model and analytical model. See text for details.

shown in Fig. 3. Here, for clarity, we have shown only the correlation signals and excluded these additional signals.

From the above simulation results, it is obvious that the numerical model and the analytical model are in good agreement with each other. Hence, we can use the analytical model reliably for simulating a three-dimensional STC. Figure 6 shows the simulation result of the STC using the analytical model [Eq. (10)], where the query event  $B(x, y, t)$  contains three frames, and the reference event  $C(x, y, t)$  contains nine reference frames. The writing frame,  $A(x, y, t)$ , and the query frames,  $B(x, y, t)$ , are centered at  $t = T_1$  and  $t = T_2$ , respectively. The section of the reference event that matches the query event is shown in the dotted box in  $C(x, y, t)$ , which is centered at  $t = T_3$ . As expected, a correlation peak appears at  $t = T_2 + T_3 - T_1$  in the  $S(x, y, t)$  signal.

So far, we have only considered a situation where the quantum state evolution can be described by the deterministic SE. However, for a system that involves non-negligible decay and irreversible dephasing, it is necessary to make use of a stochastic description. The density matrix equation of evolution for such a

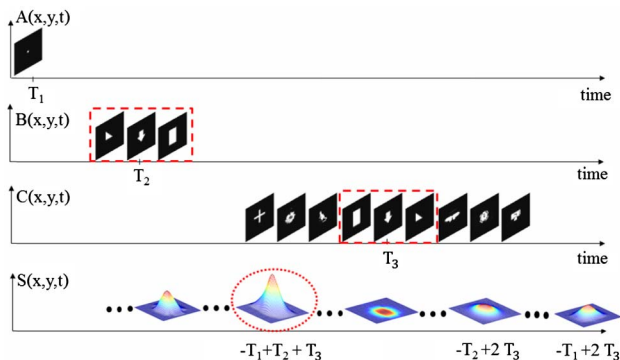


**Fig. 6.** Simulation result of the STC using the analytical model. See text for details.

system in general may not have an analytical solution as a function of time. In order to apply the technique proposed here to a such a system, we can employ the following approach. First, we develop a set of density matrix equations for each small spectral band in the STFT domain, analogous to Eq. (8), by employing the REA. In order for the REA to be valid, the width of each band has to be of the order of the homogeneous linewidth of the system. These equations, for each band, are then solved numerically in the time domain for the element of the density matrix that corresponds to the dipole moment of interest. For concreteness, consider the case of a damped two-level optical transition. In this case, the density matrix element of interest is  $\rho_{12}(k_x, k_y, \omega)$ , and the numerical solution would yield the temporal evolution of this element:  $\rho_{12}(k_x, k_y, \omega, t)$ . The desired response of the system is then found simply by integrating this quantity over the STFT domain and the spectral distribution of the atomic density:  $\rho_{12}(t) = \int d\omega dk_x dk_y N(\omega) \rho_{12}(k_x, k_y, \omega, t)$ . Computationally, this approach would be somewhat slower than an SE-based system. However, it would still be much faster than the brute-force approach of integrating over all atomic locations and frequencies. Broadly speaking, this approach is thus expected to be convenient for any situation involving the quantum evolution of a system in time and three spatial dimensions simultaneously.

#### 4. CONCLUSION

To summarize, we have developed an analytical model to find the nonlinear response of a resonant medium due to an applied field by employing the STFT-domain-based transfer function. We started with deriving the one-dimensional transfer function of an inhomogeneously broadened AM under the REA. Then, we developed the three-dimensional transfer function and showed that the analytical model agrees closely with the results obtained via an explicit simulation of the atomic response but at a speed faster than the analytical model. As a practical example of the analytical model, we showed that it can be used to model the STC at a speed that is many orders of magnitude faster than solving the SE. Finally, we also outlined how a variation of this approach can be employed for efficient computation in a system that requires the density matrix equations for the evolution of the nonlinear medium.

**Funding.** Air Force Office of Scientific Research (AFOSR) (FA9550-10-01-0288).

#### REFERENCES

1. R. Boyd, *Nonlinear Optics*, 3rd ed. (Academic, 2008).
2. L. Allen and J. H. Eberly, *Optical Resonance & Two Level Atoms* (Dover, 1987).
3. S. M. Spillane, G. S. Pati, K. Salit, M. Hall, P. Kumar, R. G. Beausoleil, and M. S. Shahriar, "Observation of nonlinear optical interactions of ultralow levels of light in a tapered optical nanofiber embedded in a hot rubidium vapor," *Phys. Rev. Lett.* **100**, 233602 (2008).
4. C. Liu, Z. Dutton, C. H. Behroozi, and L. V. Hau, "Observation of coherent optical information storage in an atomic medium using halted light pulses," *Nature* **409**, 490–493 (2001).
5. W. Tittel, M. Afzelius, T. Chanelière, R. L. Cone, S. Kröll, S. A. Moiseev, and M. Sellars, "Photon-echo quantum memory in solid state systems," *Laser Photon. Rev.* **4**, 244–267 (2010).

6. B. S. Ham, M. S. Shahriar, M. K. Kim, and P. R. Hemmer, "Frequency selective time domain optical data storage by electromagnetically induced transparency in a rare-Earth doped solid," *Opt. Lett.* **22**, 1849–1851 (1997).
7. T. W. Mossberg, "Time-domain frequency-selective optical data storage," *Opt. Lett.* **7**, 77–79 (1982).
8. L. Zhao, T. Wang, Y. Xiao, and S. F. Yelin, "Image storage in hot vapors," *Phys. Rev. A* **77**, 041802(R) (2008).
9. G. S. Pati, K. Salit, R. Tripathi, and M. S. Shahriar, "Demonstration of Raman–Ramsey fringes using time delayed optical pulses in rubidium vapor," *Opt. Commun.* **281**, 4676–4680 (2008).
10. M. S. Monjur, M. Fouda, and M. S. Shahriar, "All optical three dimensional spatio-temporal correlator for automatic event recognition using a multiphoton atomic system," *Opt. Commun.* **381**, 418–432 (2016).
11. M. S. Monjur, S. Tseng, R. Tripathi, J. Donoghue, and M. S. Shahriar, "Hybrid optoelectronic correlator architecture for shift invariant target recognition," *J. Opt. Soc. Am. A* **31**, 41–47 (2014).
12. B. S. Ham, P. R. Hemmer, M. K. Kim, and M. S. Shahriar, "Quantum interference and its potential applications in a spectral hole-burning solid," *Laser Phys.* **9**, 788–796 (1999).
13. M. S. Shahriar, Y. Wang, S. Krishnamurthy, Y. Tu, G. S. Pati, and S. Tseng, "Evolution of an N-level system via automated vectorization of the Liouville equations and application to optically controlled polarization rotation," *J. Mod. Opt.* **61**, 351–367 (2014).
14. M. S. Shahriar, P. Hemmer, D. P. Katz, A. Lee, and M. Prentiss, "Dark-state-based three-element vector model for the stimulated Raman interaction," *Phys. Rev. A* **55**, 2272–2282 (1997).
15. N. W. Carlson, L. J. Rothberg, A. G. Yodh, W. R. Babbitt, and T. W. Mossberg, "Storage and time reversal of light pulses using photon echoes," *Opt. Lett.* **8**, 483–485 (1983).
16. X. A. Shen, E. Chiang, and R. Kachru, "Time-domain holographic image storage," *Opt. Lett.* **19**, 1246–1248 (1994).
17. N. Sangouard, C. Simon, J. Minar, M. Afzelius, T. Chaneliere, N. Gisin, J. L. Le Gouet, H. Riedmatten, and W. Tittel, "Impossibility of faithfully storing single photons with the three-pulse photon echo," *Phys. Rev. A* **81**, 062333 (2010).
18. G. I. Garnaeva, L. A. Nefediev, E. N. Ahmedshina, and É. I. Akimzyanova, "Frequency-temporal correlation of inhomogeneous broadening for different modes of excitation of stimulated photon echo," *J. Appl. Spectrosc.* **81**, 944–948 (2015).
19. P. R. Hemmer, M. S. Shahriar, M. K. Kim, K. Z. Cheng, and J. Kierstead, "Time domain optical data storage using Raman coherent population trapping," *Opt. Lett.* **19**, 296–298 (1994).
20. M. G. Moore and P. Meystre, "Effects of atomic diffraction on the collective atomic recoil laser," *Phys. Rev. A* **58**, 3248–3258 (1998).
21. M. G. Moore and P. Meystre, "Theory of superradiant scattering of laser light from Bose–Einstein condensates," *Phys. Rev. Lett.* **83**, 5202–5205 (1999).
22. A. V. Oppenheim, A. V. Willsky, and S. Hamid, *Signals and Systems*, 2nd ed. (Prentice-Hall, 2010).
23. A. Renn, U. P. Wild, and A. Rebane, "Multidimensional holography by persistent spectral hole burning," *J. Phys. Chem. A* **106**, 3045–3060 (2002).
24. W. R. Babbitt, Z. W. Barber, S. H. Bekker, M. D. Chase, C. Harrington, K. D. Merkel, R. K. Mohan, T. Sharpe, C. R. Stiffler, A. S. Traxinger, and A. J. Woidtke, "From spectral hole burning memory to spatial-spectral microwave signal processing," *Laser Phys.* **24**, 094002 (2014).
25. N. Kartam and I. Flood, "Construction simulation using parallel computing environment," *Autom. Constr.* **10**, 69–78 (2000).
26. H. Adeli and O. Kamal, *Parallel Processing in Structural Engineering* (Chapman & Hall, 1993).
27. J. M. Alonso, A. Arruabarrena, R. Beivide, and J. A. B. Fortes, "An evaluation of implementations of the CMB parallel simulation algorithm on distributed memory multicomputers," *J. Syst. Archit.* **44**, 519–545 (1998).